Surface functionalization of polypropylene (PP) by chitosan immobilization to enhance human fibroblasts viability

D.S. Morais [a,b], B. Ávila [a], C. Lopes [c], M.A. Rodrigues [a], F. Vaz [c], A.V. Machado [d], M. H. Fernandes [e], R.M. Guedes [b,f], M.A. Lopes [a,],

[a] REQUIMTE-LAQV, Departamento de Engenharia Metalúrgica e Materiais, Faculdade de Engenharia, Universidade do Porto, Rua Dr. Roberto Frias, 4200-465, Porto, Portugal

[b] INEGI-Instituto de Engenharia Mecânica e Gestão Industrial, Rua Dr. Roberto Frias, 4200-465, Porto, Portugal

[c] Centro de Física, Universidade do Minho, 4710-057, Braga, Portugal

[d] IPC - Institute for Polymers and Composites, Universidade do Minho, Campus de Azurém, 4800-058, Guimarães, Portugal

[e] Faculdade de Medicina Dentária, Universidade do Porto (FMDUP), Rua Dr. Manuel Pereira da Silva, Porto, Portugal

[f] Departamento de Engenharia Mecânica Faculdade de Engenharia, Universidade do Porto, Rua Dr. Roberto Frias, 4200-465, Porto, Portugal

Keywords:

Polypropylene, PP
Chitosan
Surface functionalization
Fibroblasts
Tendon repair

Abstract

Driven by the market demand, several synthetic and natural grafts have been proposed during the last years for tendons regeneration. The synthetic grafts, which present a better mechanical performance than the natural ones, usually fail due to the lack of biocompatibility and bioactivity. Thus, chitosan (Cs) was immobilized on polypropylene (PP) surface, previously activated by plasma treatment, in order to improve the fibroblasts' adhesion and proliferation on it.

The Orange II dye method and FTIR-ATR analysis proved the successful Cs immobilization on the PP surface. It was observed by SEM and optical profilometry analysis that the Cs concentration increase leads to a surface roughness (R_a value) increase, as well as to water contact angle (C.A.) decrease at least until 2%(w/V) of Cs. Using the 2%(V/V) Cs solution concentration, according to SEM analysis and resazurin assay, the developed functionalization was well succeeded in improving fibroblasts adhesion and proliferation on PP substrates surface over 7 days of culture.

Introduction

The population aging will have a real impact on musculoskeletal health in the coming decades. In fact, musculoskeletal disorders already affect more than 100 million Europeans and this number will soon increase grounding a societal need for a regenerative medicine approach [1]. Among these disorders, tendon injuries are the most difficult to manage and although spontaneously healing can occur in some situations this often results in the formation of scar tissue, which has low functionality and consequently the tendon rupture can happen. In some cases, a simple suture backing together the tendon ends is done, but this repair practice is often ineffective. In other cases, the used approach is a tissue replacement with auto or allografts, but these reveal disadvantages, as donor site morbidity, not widely availability and rejection risk [2,3]. Driven by the market demand several synthetic and natural grafts, intended to be used as graft augmentation devices (patches) or to fully replace a damaged tendon (prostheses), have been proposed during the last years. The synthetic grafts in spite of presenting a better mechanical performance than the natural ones, they usually fail due to the lack of biocompatibility and bioactivity [4,5].

Polypropylene (PP) is a non-polar, semi-crystalline and thermoplastic polymer used for different applications, such as packaging, textiles or even for medical purposes [6,7]. Due to its hydrophobic properties, its use in several engineering applications requires functionalization aiming to increase the adhesion properties to promote its bonding ability to other polymers/resins. The traditional functionalization is based on chemical treatments but due to environmental impact, it has been moved to electrical discharge through gas followed mostly by a surface grafting step (ex poly(acrylic acid)) [8,9].

In the medical devices field, the choice of PP is usually related to their mechanical properties and safety and therefore is mainly used as suture material and meshes [10,11].

PP offers a low level of tissue reaction in contact with living tissues when compared to other synthetic polymeric materials, however, it

presents a hydrophobic profile due to the low surface energy, which may be harmful in the cell adhesion process [11-13]. Therefore, its functionalization is a benefit or even mandatory in some applications in order to change the surface properties without interfering with the mechanical resistance of the substrate. For instance coating of PP meshes to reduce the host foreign body message with porcine dermal extracellular matrix hydrogel or coating of meshed with polydopamine to carry drugs have been reported [14]. Studies of surface functionalization of PP devices aiming to improve hemocompatibility and release of antimicrobial drugs were reported by grafting N , N′-dimethylacrylamide (DMAAm) and N -isopropylacrylamide (NIPAAm) onto the surface have also been reported [15]. The clinical success in the long term of scaffolds for tendon and ligament

repair made of PP would benefit from an adequate functionalization, which is essential for tissue regeneration [16].

Many techniques such as corona discharges, ultraviolet irradiation, and plasma treatments have been used to increase its wettability [6,11, 17,18]. These techniques increase the surface free energy by incorporating oxygen-containing polar functional groups on it [11,13]. In the case of plasma treatments, the electrical energy applied from the plasma reactor dissociates the inert gas into electrons, free radicals, ions, photons, and metastable (excited) species. Those free radicals will collide with the material surface and break the covalent bonds. At that moment, the free radicals created on the material surface can combine with the air oxygen and moisture to produce thermodynamically stable functional groups on the surface. Once the plasma surface treatment affects only a limited depth (several molecular layers), the bulk properties of the material remain unchanged [11,19].

Moreover, after the plasma activation, in order to anchor active functional groups on the PP surface, specific biomolecules can be immobilized on the polymer surface to improve the device bioactivity and integration with the living tissues [20-22]. Natural polysaccharides are very promising molecules for tissue engineering applications, since they present high biocompatibility and resemble glycosaminoglycans of the extracellular matrix (ECM). These polymers have shown a lower stimulation of immunological reactions than some synthetic polymers [23]. Chitosan (Cs), for instance, which is a biodegradable polycation composed by the monomers D -glucosamine and N-acetyl-D-glucosamine linked by $\beta(1-4)$-glycosidic bond may be a good option to biofunctionalize PP substrates surface [20]. Cs properties, such as biocompatibility, low toxicity, biodegradability and promotion of cell adhesion, proliferation and differentiation, made it become a very appealing material for biomedical applications [23,24].

Therefore, the purpose of this study was to functionalize PP substrates by the immobilization of Cs on their surfaces, in order to improve the interaction of those substrates with fibroblasts for tendon tissue regeneration, or even for ligaments regeneration.

Materials and methods

Materials

The polypropylene (PP) sheets, with a thickness of 0.1 mm , were purchased from Goodfellow, acrylic acid (AAc) was supplied by Merck India Ltd. and the chitosan (MW: 100.000-300.000) and the acid orange II (99%) were purchased from Acros Organics.

Methods

PP surface plasma treatment and acrylic acid (AAc) grafting

Circular PP samples with 0.1 mm thickness and 25 mm diameter were prepared and cleaned with ethanol to be exposed to different plasma activation treatments. A Zepto laboratory-sized plasma system from Diener Electronics ($\emptyset = 105$ mm, L = 300 mm, V = 2.6 L) was used for the plasma activation of the samples. The following plasma treatments were performed according to the used gas and the plasma

treatment time, using a power of 100 W , a pressure $_{base}$ of 10 Pa and a pressure $_{work}$ of 80 Pa :

1. O_2 plasma over 2,5,8 and 10 min ;
2. Ar plasma pre-treatment over 2 min followed by O_2 plasma over 2,5, 8 and 10 min .

Subsequently, the plasma-treated samples were immersed in different acrylic acid (AAc) aqueous solutions (10% (V/V), 20% (V/V) and 40%(V/V)), at room temperature over 4 h . After the grafting reaction, to remove any non-grafted acrylic acid (AAc) distilled water was used and the samples were dried at room temperature.

Chitosan (Cs) immobilization on PP surface

The AAc treated PP samples were immersed in 10 mL of N -(3-dimethylaminopropyl)-N-ethylcarbodiimide hydrochloride (EDC) aqueous solution (concentration 10mg/mL), buffered to pH 4.8 (in sodium citrate) at $4\,^{\circ}C$ for 30 min . EDC was used to activate carboxyl groups on AAc grafted samples. The EDC-coupled samples were then immersed in 3 mL of Cs solutions, of 5 different concentrations (w/V): $0.4\%, 0.8\%, 2\%, 4\%$ and 6% and buffered to pH 4.6 using acetic acidbuffered solutions at $4\,^{\circ}C$ for 24 h . According to the combination between the AAc and Cs concentrations different samples were prepared, as described in Table 1. After the Cs immobilization, the samples were washed with acidified water at $4\,^{\circ}C$ for 30 min and dried at room temperature.

Physicochemical characterization

Fourier Transform Infrared Spectroscopy (FTIR) in Attenuated Total Reflectance (ATR) mode was performed on untreated PP samples, PP samples after each plasma treatment and after immersion in different Cs solutions (in triplicate), using the spectrometer Jasco FT/IR 4100 system (64 scans and 8 cm^{-1} nominal resolution) equipped with a Specac MkII Golden Gate single reflection ZnSe ATR crystal.

The wettability of PP samples surface after each plasma treatment and after immersion in Cs solutions was assessed by the sessile drop method ($3\mu l$ drop), measuring the water contact angle (C.A.) at room temperature, using an OCA 20 unit from Dataphysics. A minimum of 9 contact angle measurements were performed for each condition, using at least 3 samples.

The surface topography, average roughness (R_a) and surface height standard deviation (R_q) of PP substrates (2 samples of each condition) were assessed before and after the plasma activation using a Multimode Atomic Force Microscope (AFM) from Digital Instruments using the tapping mode ($5 \times 5\mu\,m^2$ scan size and 1 Hz scan rate). A Nanoscope III controller and Tesp AFM tips from Bruker were also used.

The amount of exposed amino groups on PP surfaces after Cs immobilization was assessed by the Orange II dye method, using 3 samples for each type of Cs immobilization. The samples were immersed in 3 mL of dye acidic solution (14mg/mL) (pH 3) and shaken for 5 h at $30^{\circ}C$. The samples were then thoroughly rinsed three times with water acidic solution (pH 3) to remove the unbound dye. Once air-dried, the colored samples were immersed in 2 mL of water basic solution (pH 12)

Table 1
Samples name according to the used AAc and Cs concentrations.

Samples name	AAc concentration %(V/V)	Cs concentration %(w/V)
PP_10% AAc_0.4% Cs	10	0.4
PP_10% AAc_0.8% Cs		0.8
PP_20% AAc_0.4% Cs	20	0.4
PP_20% AAc_0.8% Cs		0.8
PP_20% AAc_2% Cs		2
PP_20% AAc_4% Cs		4
PP_20% AAc_6% Cs		6
PP_40% AAc_0.4% Cs	40	0.4
PP_40% AAc_0.8% Cs		0.8

and shaken for 15 min at room temperature, measuring the absorbance of the solution at 485 nm .

Scanning electron microscopy (SEM) analysis was performed, using a FEI Quanta 400 FEG ESEM microscope, to analyze the microstructure and morphology of at least 2 samples of each Cs immobilized PP surface. The SEM images were acquired using either the secondary or the backscattered electrons mode and the elemental composition was evaluated by energy-dispersive X-ray spectroscopy (EDS). Moreover, after the Cs immobilization, the sample's surface was analyzed by optical profilometry using a Bruker NPFLEX equipment.

In vitro biological characterization

2.2.4.1. Resazurin assay. L929 Fibroblasts (ATCC CCL-1TM) were cultured in α-MEM (Gibco) supplemented with 10%(V/V) fetal bovine serum, 1% penicillin and streptomycin solution (Gibco) and 2.5μ g/mL of fungizone (Gibco). Cells were seeded at 2×10^4 cells per well (24 -well culture plates) on the surface of the sample (untreated PP substrate and Cs functionalized PP substrate) for 1,3 and 7 days at $37\,^{\circ}C$, in a $5\%CO_2$ humidified atmosphere. After each time point, 50μl of resazurin (SigmaAldrich) at $37^{\circ}C$ was added to each well and the plates were incubated for 3 h at $37\,^{\circ}C$ in a $5\%CO_2$ humidified atmosphere. Then, the fluorescence (excitation: 530 nm ; emission: 590 nm) was measured in a microplate reader (Synergy HT, Biotek). This experiment was performed in triplicate for each different material and at each time point. Moreover, at each time-point, following the resazurin assay, which is a nondestructive cell assay, the colonized material samples were stained by the MTT reduction assay allowing the visualization of the cell layer by optical microscopy. In this assay, cultures were incubated with MTT solution (3-[4,5-dimethyl-thiazol-2-yl]-2,5-diphenyltetrazolium bromide, Sigma-Aldrich; 5mg/mL) for 3 h . Viable cells reduced the MTT reagent to a blue formazan compound that precipitates inside cells, allowing the visualization of the cell layer by optical microscopy.

2.2.4.2. SEM analysis. The morphology of L 929 fibroblasts seeded on the surface of untreated PP samples and Cs functionalized PP samples, after each time point, was analyzed in triplicate by SEM using a FEI Quanta 400 FEG ESEM microscope. Briefly, samples with cells were firstly washed twice with PBS and fixed with 1.5%(m/V) glutaraldehyde in 0.14 M sodium cacodylate buffer (pH 7.4) over 15 min . Afterward, samples were dehydrated using graded ethanol solutions from 50% (V/ V) to 100%(V/V). The samples lasted 10 min in 70 and 80% ethanol solutions, 20 min in 90% ethanol solution and overnight in 100% ethanol solution. Finally, samples were sputter-coated (SPI-Module) with a thin gold/palladium film and visualized.

Statistical analysis

Experimental data are presented as mean ± SD (standard deviation). Statistical analysis of data was performed using the one-way ANOVA test with Bonferroni post hoc analysis, using the software SigmaStat 3.5. The differences were considered to be significant at a level of $p < 0.05$.

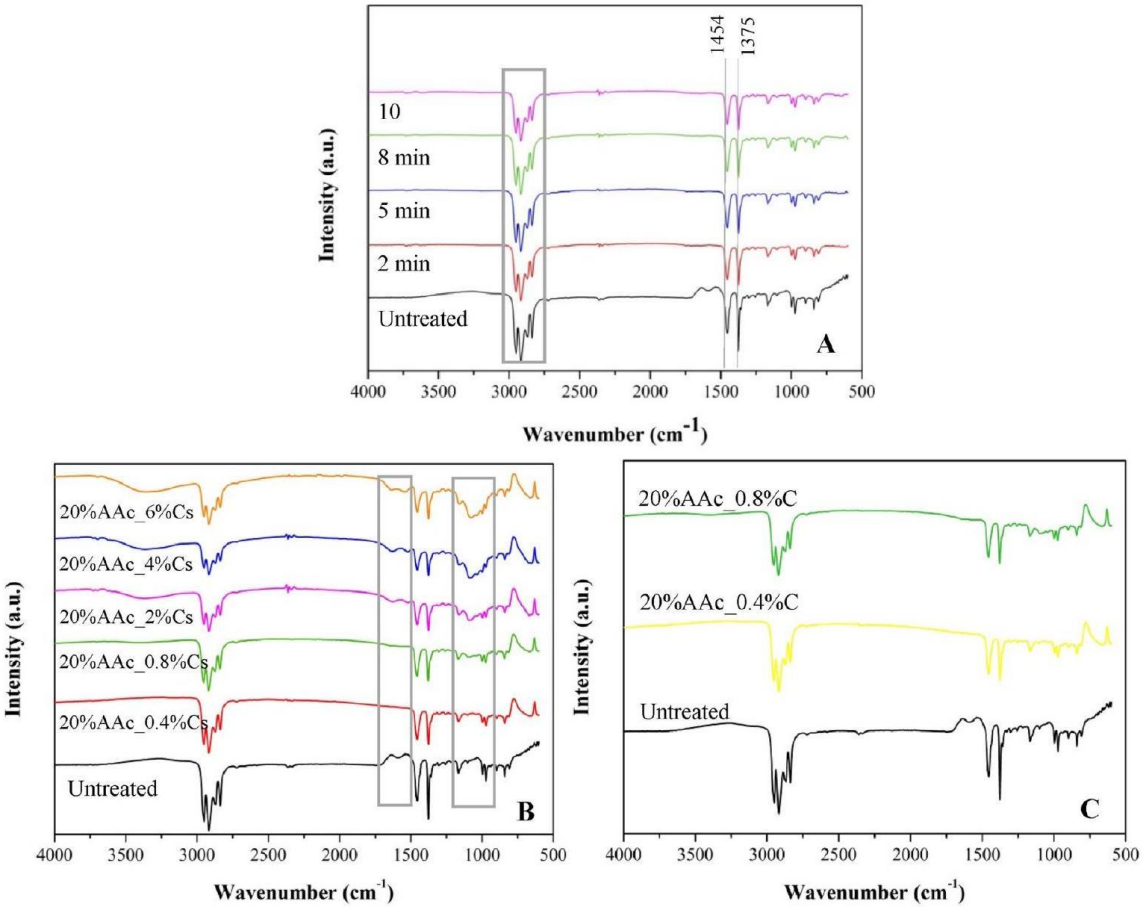

Fig. 1. FTIR-ATR spectra of the untreated PP surface, Cs powder and PP samples surface after: (A) exposure to O_2 plasma over different times; (B) exposure to O_2 plasma over 5 min and treatment with 20%AAc and different Cs concentrations; (C) exposure to Ar pre-treatment over 2 min followed by O_2 plasma over 5 min and treatment with 20%AAc and two different Cs concentrations.

Results

PP surface plasma treatment

FTIR-ATR analysis

In order to evaluate the chemical groups presented on surface of untreated PP samples and PP samples exposed to different times of plasma O_2 plasma, FTIR-ATR analysis was performed, as presented in Fig. 1A. Using this technique no detectable changes were observed among spectra before and after exposure to the different plasma treatments. For all samples, it is possible to observe characteristic peaks of PP in the region 3000-2800 cm^{-1}, namely at 2951 cm^{-1}, 2916 cm^{-1}, 2871 cm^{-1}, and 2836 cm^{-1}. Moreover, two other intense peaks were observed at 1454 cm^{-1} and 1375 cm^{-1}. Regarding the *Ar* plasma pre-treatment over 2 min followed by O_2 plasma over different times, the FTIR-ATR analysis was also performed (data not showed) and also no detectable changes were observed before and after plasma exposure.

Wettability evaluation

In Fig. 2A it is possible to observe the water C.A. variation after exposure to O_2 plasma over different times and to the Ar pre-treatment over 2 min followed by different times of O_2. The presented results show for both plasma compositions (O_2 and Ar pre-treatment followed by O_2)

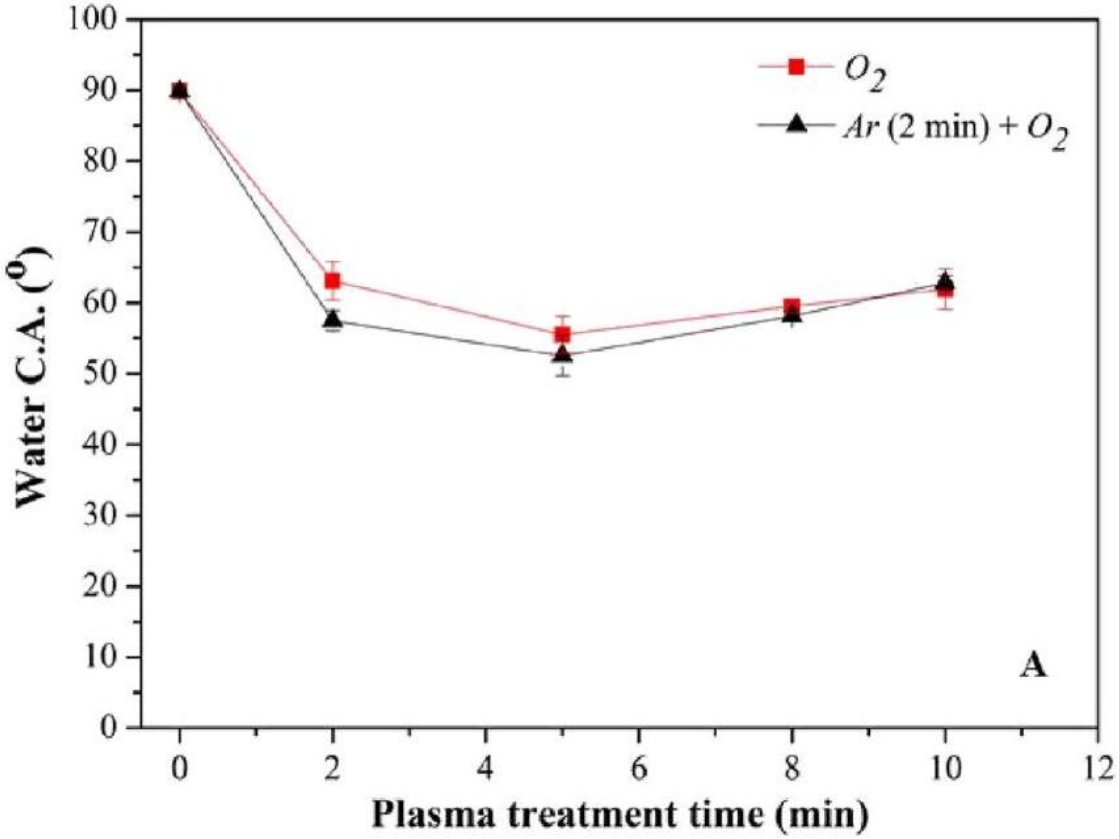
100
90
80
70
60
50
40
30
20
10
0
Water C.A. (°)
O_2
Ar (2 min) + O_2
A
0
2
4
6
8
10
12
Plasma treatment time (min)

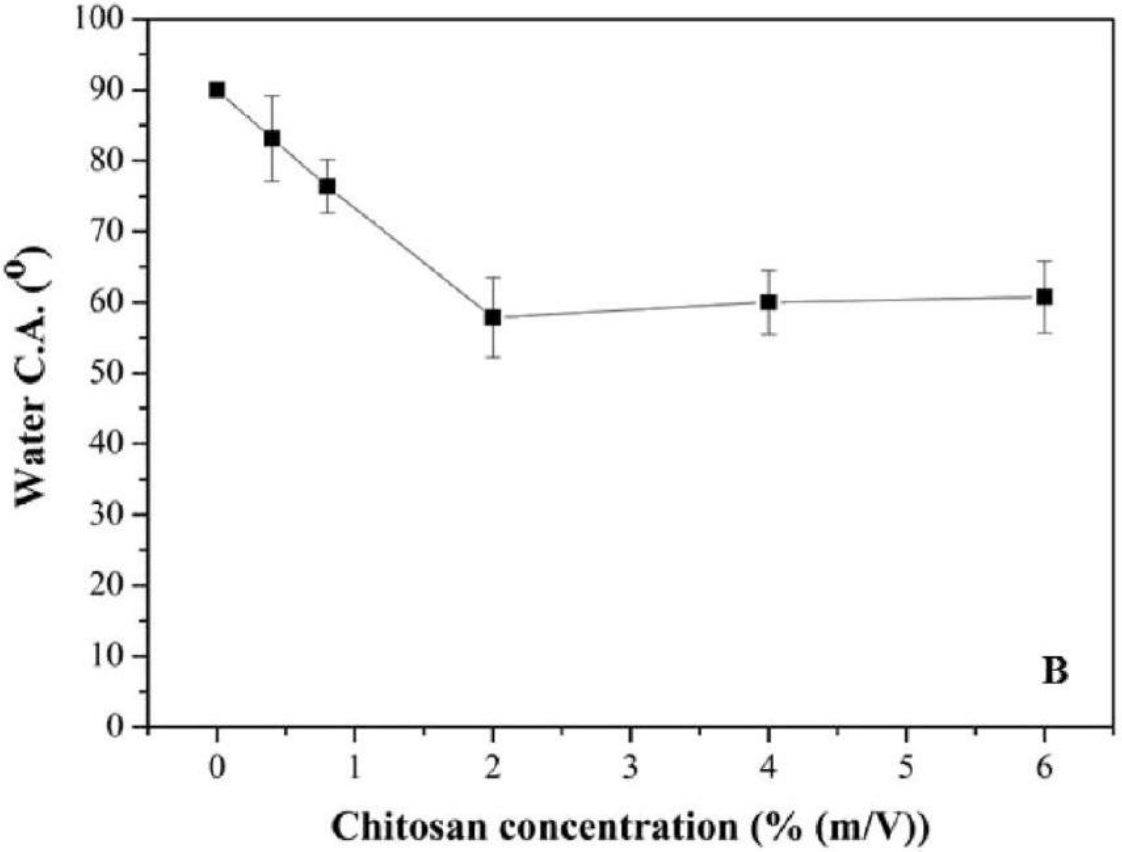
100
90
80
70
60
50
40
30
20
10
0
Water C.A. (°)
B
0
1
2
3
4
5
6
Chitosan concentration (% (m/V))

Fig. 2. Water C.A. variation on the PP surface after: (A) exposure to O_2 plasma over different times and to the Ar pre-treatment over 2 min followed by different times of O_2; (B) functionalization with different Cs concentrations after the O_2 plasma treatment over 5 min and 20% AAc grafting.
a significant C.A. decrease after 2 min of plasma exposure. However, C. A. values reached the lowest levels after 5 min of treatment, being observed a decrease from $89.8° \pm 0.2$ (untreated PP) to about $55.5° \pm 2.6$ in case of O_2 plasma treatment over 5 min and $52.5° \pm 2.9$ for the Ar pre-treatment over 2 min followed by O_2 plasma treatment over 5 min , representing for both cases a decrease of about 41%. But after the 5 min the water C.A. slightly increases again.

AFM analysis

AFM analysis was performed in order to evaluate the effect of plasma treatment on PP surface roughness. Table 2 shows the average roughness (R_a), root mean square roughness (R_q) and representative 3D height images for untreated PP, after the O_2 plasma treatment over 5 min and after the Ar pre-treatment over 2 min followed by O_2 plasma over 5 min . As observed, the untreated PP sample surface shows a heterogeneous rough surface with high protuberances. After the O_2 plasma, a nonuniform rough topography is still observed. However, the $Ar(2\ min) + O_2(5\ min)$ treatment caused a very less rough and more homogeneous surface, which presents similar peaks and valleys of low amplitude uniformly distributed. Moreover, the quantification of the roughness values indicates that when the PP surface is exposed only to O_2 plasma, the R_a value decreases from 21.5 nm to 17.7 nm and when it is exposed to $Ar(2\ min) + O_2(5\ min)$ the R_a value decreases to 11.7 nm . As presented the R_q value also decreases after both plasma treatments, namely from about 30.5 nm to about 23.1 and 15.1 nm . According to the representative images, the topography of the plasma-treated surfaces seems to be more homogenous, presenting similar peaks and valleys uniformly distributed on the surface.

CS immobilization on PP surface

Physicochemical characterization

3.2.1.1. Orange II dye method. Fig. 3A presents the acid orange absorbance levels of PP samples previously exposed to different plasma compositions and subsequently immersed in AAc solutions with different concentrations and finally immersed in two distinct Cs solutions. When a plasma treatment only based on O_2 is performed, the absorbance level tends to increase as the function of AAc concentration until the 20% AAc, after that it stabilizes. When using Ar plasma pretreatment followed by O_2 plasma, the absorbance level also tends to increase as a function of AAc concentration until the 20% AAc, but after that, there is an absorbance decrease. For a specific plasma treatment and specific AAc concentration, for instance, at 20%(V/V) where the absorbance level of all conditions reaches its maximum, the absorbance is the highest when using the highest Cs concentration (0.8%). When comparing the maximum absorbance achieved using a specific AAc and Cs concentration, but using different plasma treatments, no significant difference is observed. Fig. 3B shows the acid orange absorbance of PP samples after exposure to O_2 plasma over 5 min and subsequent treatment with 20% AAc and different Cs concentrations. It is possible to observe that the absorbance level rises as the Cs concentration increases, however, the increment is less significant after the 2%Cs.
3.2.1.2. FTIR-ATR analysis. In Fig. 1 B and 1 C , it is presented the FTIRATR spectra of

untreated PP and PP samples after Cs immobilization using different concentrations. It must be referred that the Cs powder spectrum was also acquired to identify the typical peaks, however, the spectrum is not showed. Fig. 1 B concerns to samples activated with 0_2 plasma over 5 min and grafted with 20% AAc and Fig. 1C concerns to samples subjected to the Ar pre-treatment over 2 min followed by 0_2 plasma over 5 min and grafted with 20% AAc. revealed its typical broad peaks with a very low intensity, being difficult to identify them with the used graph scale. When using the Ar pre-treatment followed by 0_2, there is any visible change in spectra comparing the untreated PP with Cs

Table 2
Representative AFM micrographs and roughness parameters (R_a and R_q) of untreated PP surface and after exposure to different plasma conditions.

Sample	Surface micrograph	R_a(nm	R_q(nm
Untreated PP	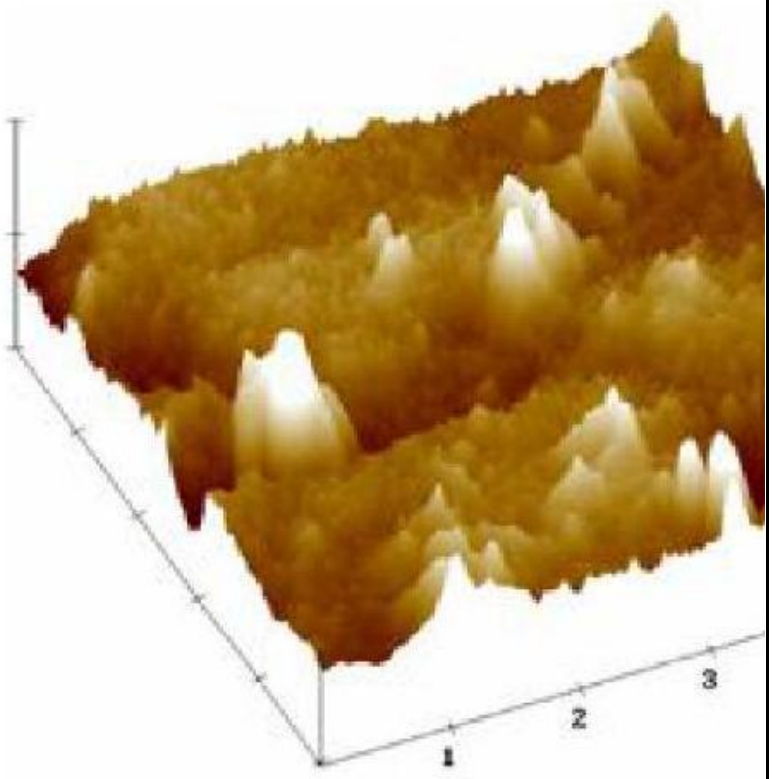	21.5 $\pm$ 1.3	30.5 $\pm$ 1.6

O_2 plasma over 5 min	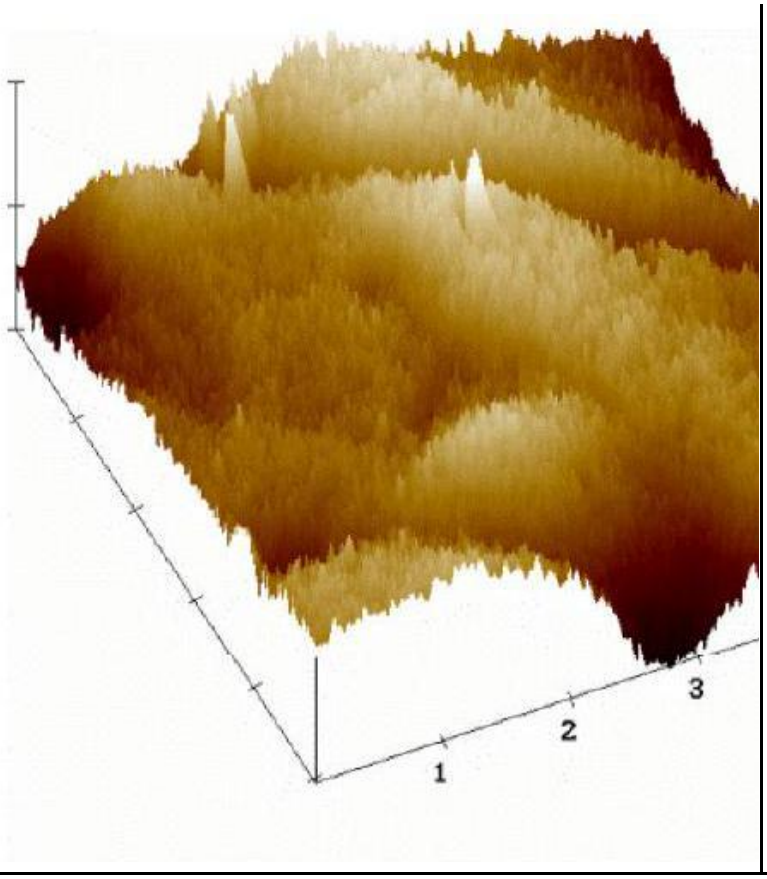	17.7 $\pm$ 1.8	23.1 $\pm$ 2.1

Ar plasma pre-treatment over 2 min followed by O_2 plasma over 5 min	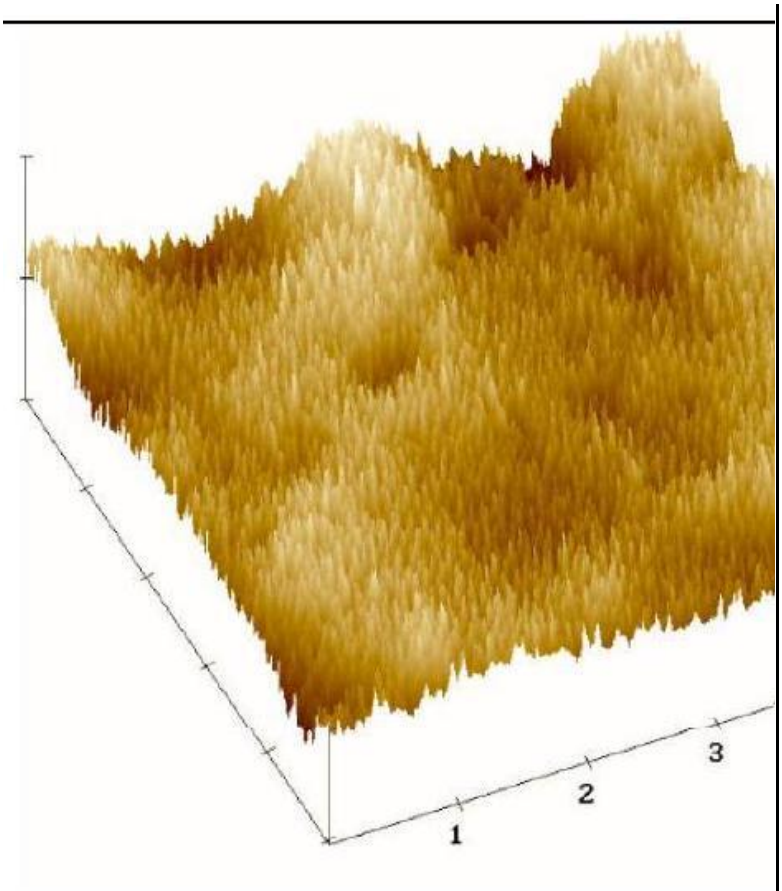	11.7 $\pm$ 1.8	15.1 $\pm$ 2.5

treated PP. When using only O_2 plasma, for the higher Cs concentrations (2%, 4% and 6%(w/V)) a new broad peak of very low intensity is visible between 3000 cm^{-1} and 3600 cm^{-1} and other two peaks of low intensity appear around 1637 cm^{-1} and 1164 cm^{-1} (as assigned in Fig. 1B).

3.2.1.3. SEM analysis. SEM analysis was performed in order to evaluate the PP surface morphology before and after Cs immobilization on it, using different Cs concentrations, after exposure to O_2 plasma over 5 min and 20% AAc grafting. The untreated PP sample (Fig. 4A) revealed a uniform surface, being possible to observe some crystallite boundaries. When the 0.4%Cs is immobilized on PP surface (Fig. 4B) those boundaries are less visible, getting unnoticeable when using 0.8%Cs (Fig. 4C), where some kind of film seems to be deposited on the material surface. Moreover, for the two highest Cs concentrations (Fig. 4D and 4E) the boundaries are also completely unnoticeable, but the surface seems rougher, mostly in the case of 4%Cs, where some agglomerates are observed.

3.2.1.4. Optical profilometry analysis. The surface topography of PP samples functionalized with different Cs concentrations (after O_2 plasma and 20% AAc grafting) was investigated by optical profilometry (Fig. 5). It might be noticed that the Cs functionalized surfaces were washed

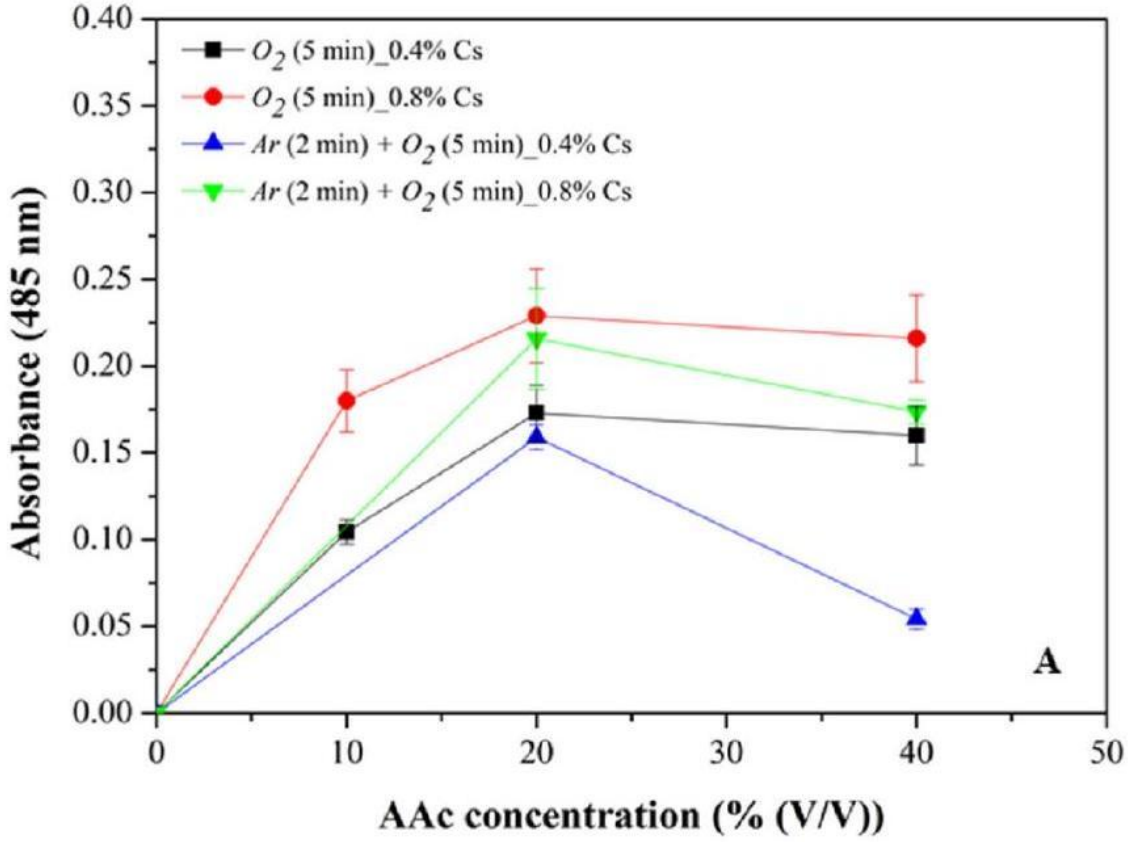
O_2 (5 min)_0.4% Cs
O_2 (5 min)_0.8% Cs
Ar (2 min) + O_2 (5 min)_0.4% Cs
Ar (2 min) + O_2 (5 min)_0.8% Cs
Absorbance (485 nm)
AAc concentration (% (V/V))
A

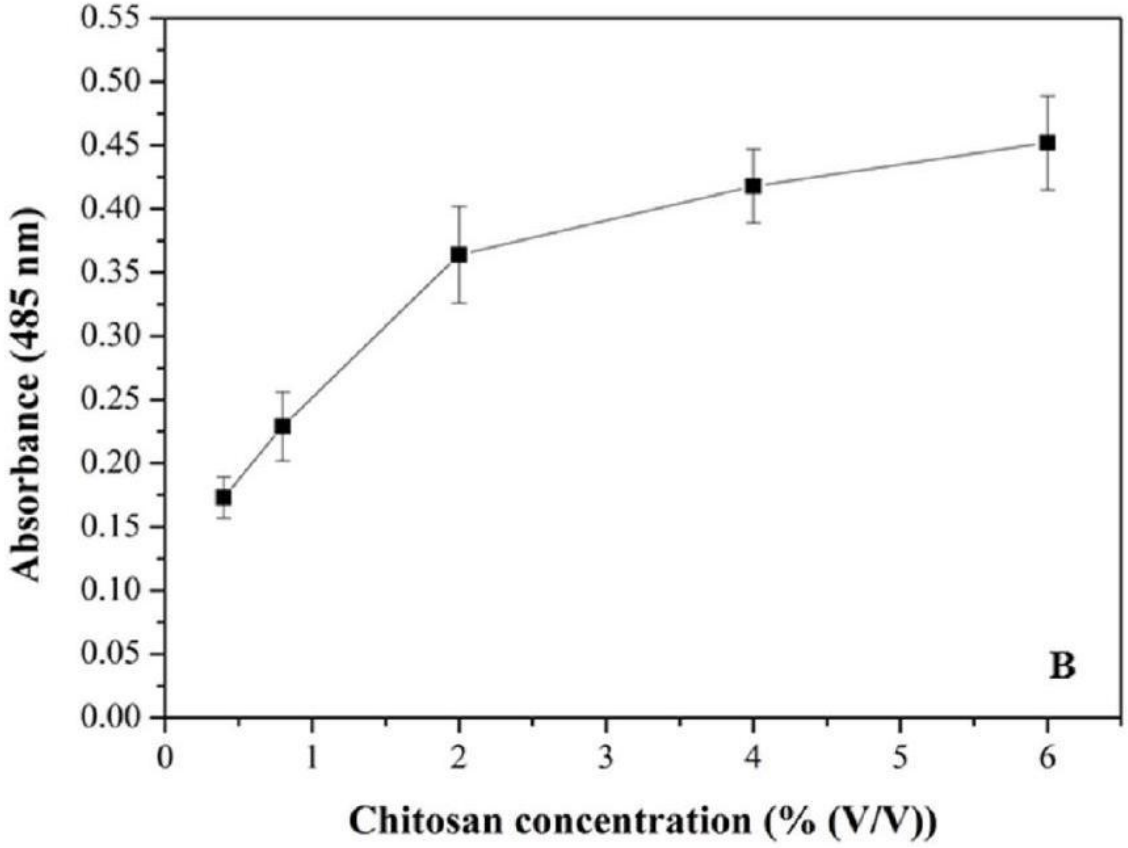
Absorbance (485 nm)
Chitosan concentration (% (V/V))
B

Fig. 3. Levels of acid orange absorbance: (A) for four different samples exposed to different plasma treatments and immersed in different Cs solution concentrations, as function of the AAc solution concentration; (B) for different Cs concentrations after the O_2 plasma treatment over 5 min and 20%AAc grafting. (For interpretation of the references to color in this figure legend, the reader is referred to the Web version of this article.)

under acidic conditions to remove any physically trapped CS on the sample surface. The untreated PP surface (Fig. 5A) shows a surface with occasional protuberances, presenting a R_a value of about 54 nm . After Cs immobilization, the surface roughness of PP_20% AAc_0.4% Cs and PP_20% AAc_0.8% Cs (Fig. 5B and C), does not suffer a significant change, presenting R_a values of about 48 and 55 nm , respectively. When the Cs concentration increases to 2% and 4%(w/V) more protuberances appear on the surface, which is reflected in an increase of the R_a value to about 99 and 135 nm , respectively (Fig. 5D and E).

3.2.1.5. Wettability evaluation. In Fig. 2*B* it is possible to observe the water C.A. variation with Cs concentration, using 20%AAc, where it is observed that the C.A. value decreases as the Cs concentration increases until 2%(V/V). Comparing the water C.A. of the untreated PP surface with the PP_20% AAc_2% Cs there is a significant decrease of about 36.5%, from about $89.8° \pm 0.2$ to $57° \pm 6$. For Cs concentrations higher than 2%(V/V) there is a stabilization of the C.A. value.

In vitro biological characterization

3.2.2.1. Resazurin assay. The metabolic activity of fibroblasts seeded on the untreated PP samples and PP samples treated with 20% AAc_2% Cs (pre-treated with 0_2 plasma) was evaluated and compared by the resazurin assay over 7 days of culture. As observed in Fig. 6A, in the case of untreated PP, the resazurin fluorescence increases over time. Over the treated PP, there is an increase in fluorescence from day 1 to day 3, being the values at both time points higher than those of untreated PP. However, on day 7 the fluorescence decreases being the value lower than that for the untreated samples.

At each time-point, following the resazurin assay, the cultured materials were stained by the MTT assay. Fig. 6B, C and D show the metabolic viable cell layer (stained blue) grown on the treated PP surface over time. It is clearly observed that the number of stained cells increased greatly from day 1 to day 3 (in line with that observed in the resazurin assay). It is also evident that, on day 3, the material surface was completely covered by a cell layer (Fig. 6C). From this stage on, space is no more available to support cell growth and, progressively, the cell layer is becoming senescent and detach from the material surface, as observed at a 7-day time-point (Fig. 6D). This explains the lower values measured in the resazurin assay on day 7 (Fig. 6A).

3.2.2.2. SEM analysis. In Fig. 7 it is possible to observe the cells seeded on the untreated PP surface (Fig. 7A1 and A2) and on the PP surface treated with 20% AAc_2% Cs (pre-treated with O_2 plasma) (Fig. 7B1 and B2) after 1 and 7 days of culture. After 1 day of incubation, it is possible to observe that fibroblasts adhered to the untreated and treated samples surfaces, even though the cells present different morphologies in each material, as observed in Fig. 7A1 and B1. On the untreated surface, some cells present a spherical morphology, while other cells present a more spread morphology. On the treated samples surface, besides the higher number of cells, all of them already present a spread shape with developed filopodia. After 7 days of incubation, Fig. 7A2 and B2 illustrate an increase in the number of cells adhered to the materials surface comparing to day 1 . Both materials surface is completely covered by an abundant cell layer, where all cells are completely spread and interconnected as a whole.

Discussion of results

In order to improve the fibroblasts' interaction with PP substrates for tendons regeneration, an efficient protocol was developed and optimized to functionalize the PP surface by Cs immobilization on it. In order to promote a strong bond (covalent bond) between the immobilized Cs and the PP surface, the substrates were first exposed to plasma treatment and acrylic acid (AAc) grafting. First of all, the activation of the PP surface with oxygen-containing plasma generates oxygenated species on the surface, within a very short exposure time [21,24,25]. After that, the grafting of AAc may be initiated, but the plasma treatment parameters and reaction conditions significantly influence the AAc grafting degree, which subsequently defines the physicochemical features at the surface [10]. The AAc grafting introduces carboxyl groups (-COOH) on samples surface for the binding of Cs through a dehydration reaction mediated by EDC, promoting a covalent amide bonding (RCONHR'6 ring) between amino groups ($-NH_2$) of Cs and carboxyl groups grafted on PP surface [10].

Based on previous studies (not yet published), the studied plasma treatments included only O_2 plasma, which is essential to activate the surface, improve its hydrophilicity and AAc grafting, or Ar followed by 0_2, once that Ar can eliminate possible contaminations from the surface and homogenize it before the treatment, improving the activation [6, 26]. To optimize the parameters of the surface activation process, several treatments using those two plasma compositions were carried out at different exposure times. In Fig. 1A, it is possible to observe the fingerprinting peaks of untreated PP. The peaks at 2951 cm^{-1} and 2871 cm^{-1} are due to the asymmetric and symmetric stretching vibrations of methyl group ($-CH_3$), respectively. The peaks at 2916 cm^{-1} and 2836

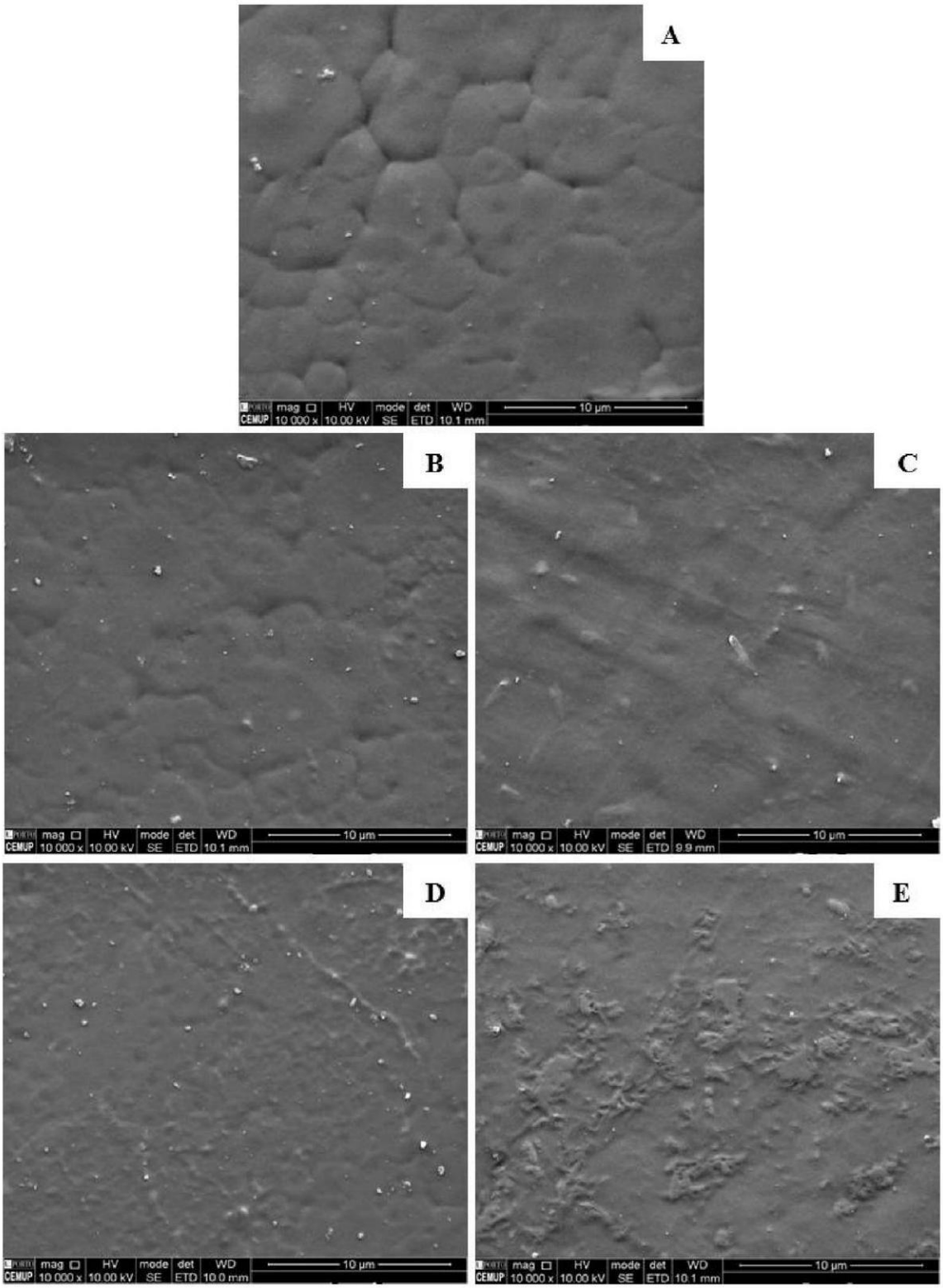

Fig. 4. SEM images of PP samples surface: (A) untreated PP; (B) PP treated with 20% AAc_0.4% Cs; (C) PP treated with 20% AAc_0.8% Cs; (D) PP treated with 20% AAc_2% CS and (E) PP treated with 20% AAc_4% CS.

cm^{-1} may be ascribed to the $-CH_2$ asymmetric and symmetric stretching vibrations,

respectively [10]. Moreover, the two peaks at 1454 cm^{-1} and 1375 cm^{-1} are related to the asymmetric and symmetric bending vibrations of $-CH_3$, respectively [27]. After the different plasma treatments, no new peaks were detected by the FTIR-ATR analysis.

The plasma activation of the PP surface was mainly performed to improve its wettability and consequently allow a better diffusion of the AAc water solution, achieving a better grafting degree, by introducing on PP surface new functional groups, such as carboxyl (-COOH) and hydroxyl (-OH), which may increase its surface hydrophilicity [11,13, 27]. However, these new groups may not have been detected in FTIR-ATR analysis due to their low quantity on the surface be under the minimum limit of detection. According to the results in Fig. 2A, the water C.A. significantly decreases as the exposure time to both plasma compositions increase, at least until 5 min , but then it slightly increases again. The Wenzel's model ($\cos(\theta W) = r\cos(\theta Y)$) describes the relationship between the apparent C.A. on a rough surface (θW), the surface average roughness ratio (r , the ratio between the real and geometric area) and the C.A. on a chemically similar smooth surface (θ Y) [6,28]. The wettability of surfaces is simultaneously related to the chemical and topographic changes promoted by the plasma treatments. According to the model and as reported by other authors, the wettability increase is usually associated with a R_a value increase due to a surface area increase (considering that no chemical changes happened) [6,29]. However, observing Fig. 2A and Table 2, in this study the PP surface wettability increases when the R_a value decreases. Therefore, taking the Wenzel's model in consideration, the water C.A. decrease may eventually be accomplished by chemical changes on the surface promoted by the plasma treatments, namely by the introduction of new chemical polar groups, as other authors have already reported [21,27,29]. Those polar groups, namely oxygen-containing polar functional groups will also allow the AAc grafting. As the exposure time to O_2 increases the surface concentration of polar functional groups also increases, leading to an improvement of surface hydrophilicity. However, after some exposure

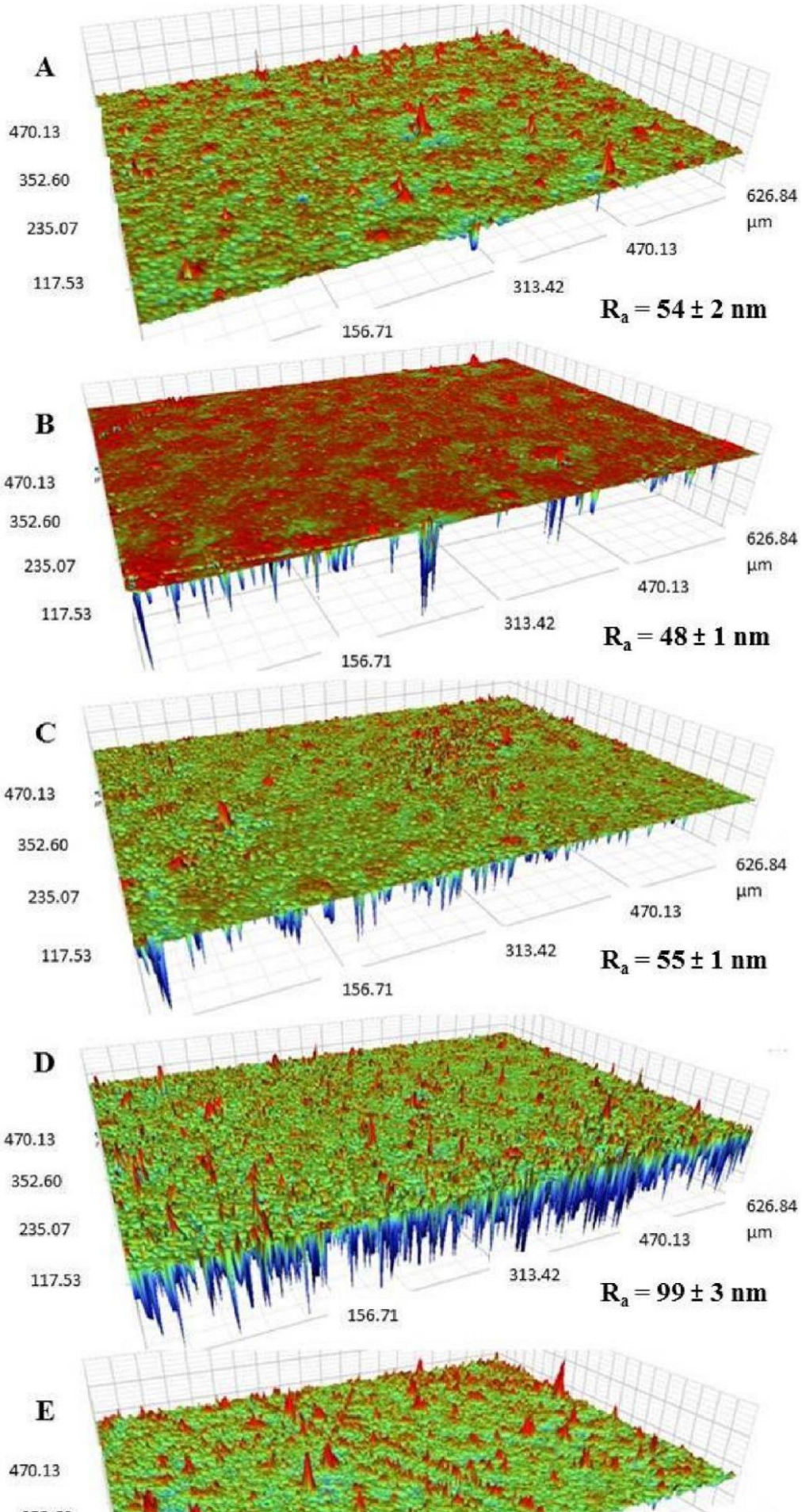
A
470.13
352.60
235.07
117.53
156.71
313.42
470.13
626.84
µm
$R_a = 54 \pm 2$ nm
B
470.13
352.60
235.07
117.53
156.71
313.42
470.13
626.84
µm
$R_a = 48 \pm 1$ nm
C
470.13
352.60
235.07
117.53
156.71
313.42
470.13
626.84
µm
$R_a = 55 \pm 1$ nm
D
470.13
352.60
235.07
117.53
156.71
313.42
470.13
626.84
µm
$R_a = 99 \pm 3$ nm
E
470.13

Fig. 5. Representative optical profilometry images of PP samples surface and R_a values: (**A**) untreated PP; (**B**) PP treated with 20% AAc_0.4% Cs; (**C**) PP treated with 20% AAc_ 0.8% Cs; (D) PP treated with 20% AAc_2% CS and (E) PP treated with 20% AAc_4% CS.

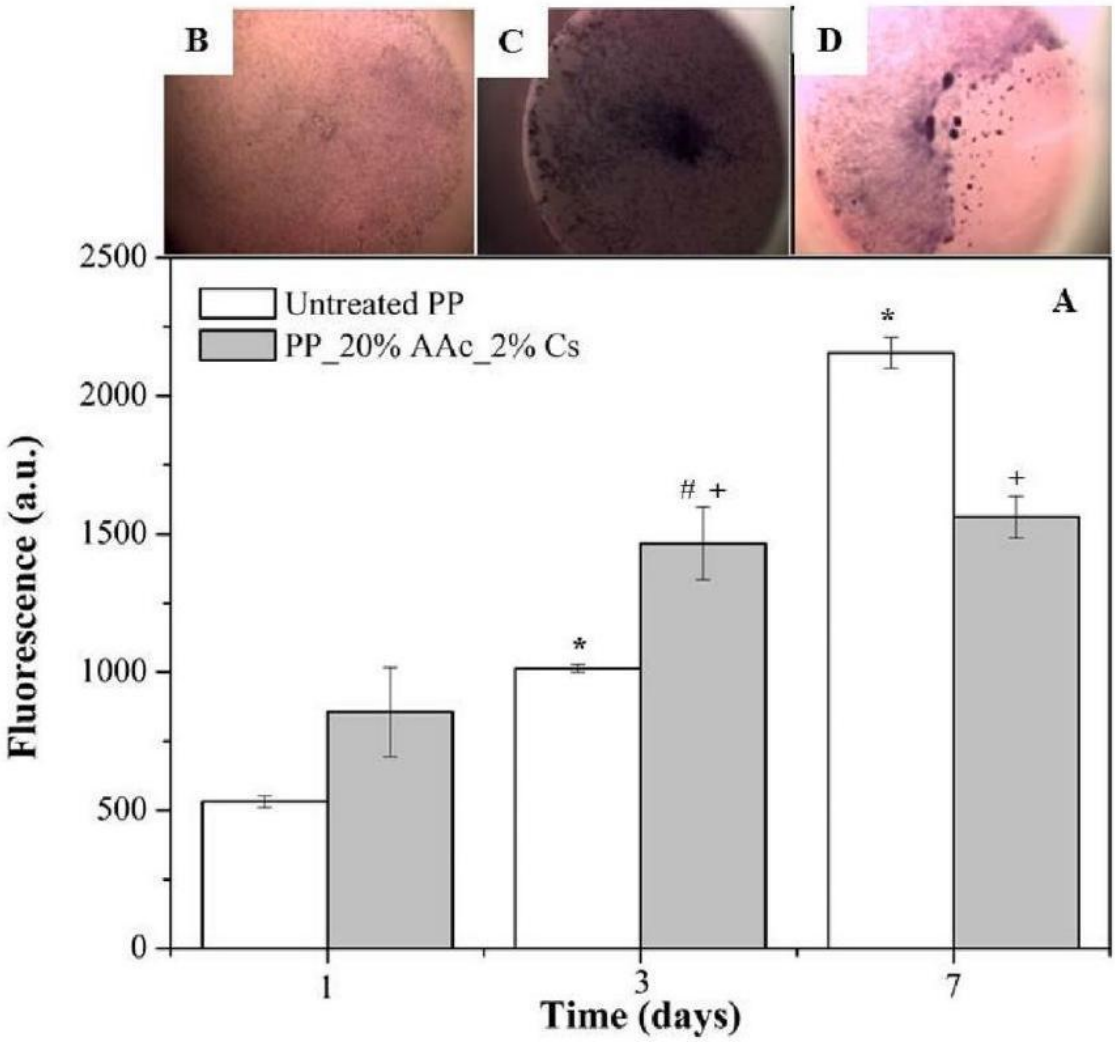

Fig. 6. Levels of resazurin fluorescence at different incubation time points after the cell seeding on untreated PP samples and PP_20% AAc_2% Cs samples (A). Microscopic images of viable cells stained by the MTT assay (blue staining) seeded on PP_20% AAc_2% Cs samples after: (B) 1 day; (C) 3 days and (D) 7 days of incubation. Data are presented as mean ± SD. $p < 0.05$-significant difference comparing untreated PP over time (*); comparing PP_20% AAc_2% Cs over time (+); comparing the untreated PP with PP_20% AAc_2% Cs at day 3 (#).

time (in this case after 5 min) an etching phenomenon may happen, leading to the removal of some weakly bonded oxide compounds or breakage over-layers on the PP surface, resulting in a decrease of polar groups present on the surface and of course of its hydrophilicity [11]. Even regarding the surfaces roughness after plasma treatment, besides

the decrease of the average roughness (R_a), it must be noticed the R_q value decrease, what indicates that the surface became more homogeneous in accordance to what is observed in images presented in Table 2 [30].

As observed in Table 2, after O_2 plasma treatment a heterogeneous rough topography was observed, being evident a hill/valley structure with a R_a value slightly lower than in untreated PP, as observed by other authors [31,32]. But when $Ar(2\ \mathrm{min}) + O_2(5\ \mathrm{min})$ treatment is performed, the surface becomes less rough and more homogeneous. The roughness change is mostly promoted by the plasma physical etching on the surface. Therefore, the different topography between the two used plasmas may be explained by the atoms (Ar and O_2) radius difference.

In order to evaluate the Cs immobilization degree on PP surface, depending on plasma composition (the 5 minO_2 plasma activation was chosen due to the low water C.A.), AAc grafting and Cs concentration, the Orange II dye method was performed, being the acid orange absorbance proportional to the $-NH_2$ groups density on the functionalized surface [33]. As presented in Fig. 3A, until 20% (V/V), the AAc concentration increase leads to an increment of $-NH_2$ groups number for both plasmas and Cs concentrations. After plasma activation, the AAc grafting degree will be as higher as the AAc solution concentration. A higher grafting degree means a higher number of -COOH groups on PP surface available to react with $-NH_2$ groups, allowing the immobilization of more Cs. For a specific plasma treatment and AAc concentration, the $-NH_2$ groups density increases as Cs concentration increases (from 0.4% to 0.8%), indicating that with 0.4%Cs several -COOH groups were still available to receive more $-NH_2$ groups. Thus, when the Cs concentration goes up to 0.8%, more Cs is immobilized on the PP surface.

However, when using the O_2 plasma treatment the absorbance level remains constant for AAc concentrations higher than 20%(V/V). This is the indication that the interaction of $-NH_2$ groups of Cs with -COOH groups may be saturated, which may be due to the occupation of all -COOH groups or due to the limited Cs chains accessibility to the AAc grafted layer. According to Saxena et al., as the -COOH content increases the amide fraction decreases revealing that the interaction of Cs molecules with the AAc grafted chains becomes difficult as the graft level increases. This phenomenon may be understood by the fact that Cs is a long-chain polysaccharide and its mobility within the AAc grafted domain on the sample surface would be a key factor in its bonding ability with -COOH groups. The grafted AAc chains are hydrophilic in nature and tend to swell when the sample is immersed in the Cs solution and at low AAc graft levels the chains are shorter but for higher graft levels the chains become longer, which may difficult the Cs chains movement and hence restrict its interaction with the -COOH groups.

When an Ar pre-treatment is performed for the PP surface activation, for AAc concentrations higher than 20%(V/V) the amines density is lower than those observed when using only O_2 plasma treatment. This lower density may happen because the O_2 reactive plasma concentration in the chamber will be lower due to the space occupied by the residual Ar particles and to the higher molecular weight of Ar, which may hamper the O_2 entrance in the next 5 min into the chamber, being present in less quantity. Moreover, O_2 atoms are quite reactive and withdraw electrons from other gases on account of their relatively high electro-negativity. Thus, in the presence of Ar atoms, the O_2 plasma density becomes low because O_2 acts as an electron and radical scavenger. Some of the electrons and free radicals lose their energy for surface activation because energy transfer, such as the adsorption, collision, and excitation, occurs through a reaction between O_2 and other

electrons and free radicals [11]. As consequence, the number of activated sites on the surface, for later AAc grafting, is lower than using only O_2 plasma, which consequently decreases the number of carboxylic groups available to react with Cs amino groups.

According to these results, the 20% AAc grafting and the plasma composed only by O_2 were chosen to study if the Cs immobilization degree could be improved by increasing Cs solution concentration, as presented in Fig. 3B. As already discussed, the increase in acid orange absorbance, from the 0.8%Cs to 2%Cs, reveals that more Cs is immobilized on the PP surface, meaning that the grafted surface still has -COOH groups available to react with $-NH_2$. However, when the Cs concentration increases to 4% and 6%, the absorbance increase is not significant. This may be explained by the fact that there are no available -COOH groups to interact with all Cs in solution or the Cs mobility may become more difficult attending to the increase of Cs solution viscosity.

In accordance with the acid orange absorbance results, the FTIR-ATR spectra of the PP surface after Cs immobilization (Fig. 1B and 1C), described new peaks when using O_2 plasma treatment and for the higher Cs concentrations. The new broad peak of very low intensity between 3000 cm^{-1} and 3600 cm^{-1} may represent the hydrogen-bonded OH stretching from the carboxyl groups [34,35]. This may prove the presence of -COOH groups on the PP surface due to AAc grafting. The appearance of this peak only for higher concentrations may be explained, as already mentioned, by the difficulty of Cs chains movement, leaving some -COOH groups unoccupied. The other two peaks observed around 1637 cm^{-1} and 1164 cm^{-1} should be related to the $C=O$ stretching vibration of amide (RCONHR'6 ring) and $C-N$ stretching vibration of amine I ($R-NH_2$) respectively, which may not be detectable by FTIR analysis above a certain density. The amide characteristic peak confirms the presence of $-CONH-$ bonds on the PP surface, indicating that the Cs (- NH_2 groups) were successfully linked to the AAc grafted PP surface (-COOH groups). Regarding the amine peak, when the Cs is immobilized on PP surface some of its $-NH_2$ groups are involved in -CONH- bonds forming amides, but other ones are kept in their amine state, as identified by the FTIR analysis. The absence of these new peaks when an Ar pre-treatment is performed is probably due to a lower density of functional groups, being not possible to detect them by

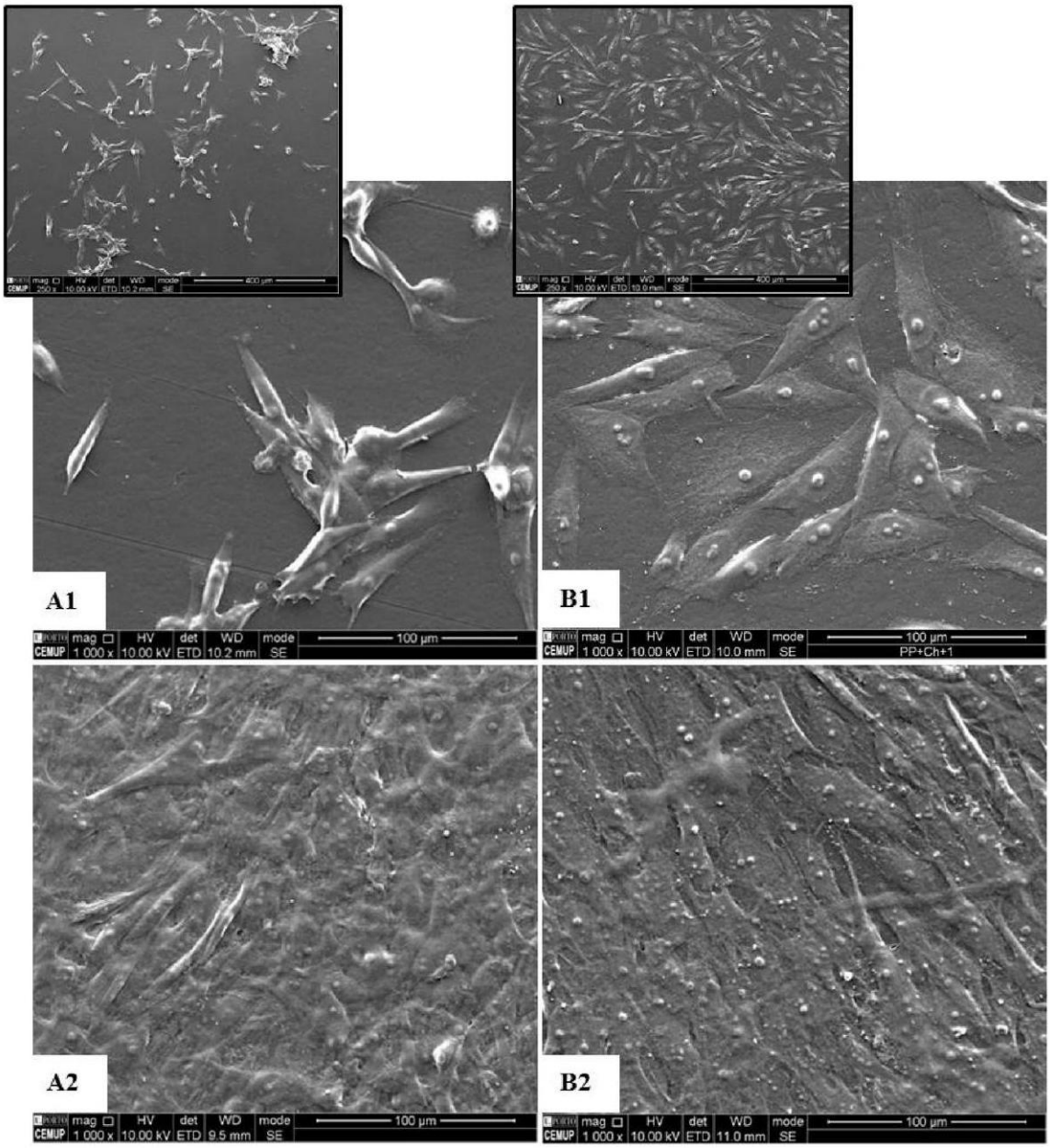

Fig. 7. SEM images of cells seeded on PP samples surface over incubation time: (A1) untreated PP after 1 day; (A2) untreated PP after 7 days; (B1) PP treated with 20% AAc_2% Cs after 1 day and (B2) PP treated with 20% AAc_2% after 7 days.

FTIR analysis.

Attending to the previous results, a further characterization by SEM, optical profilometry, and wettability analysis was performed only for samples in which the surface activation was promoted using a plasma treatment composed by 0_2 followed by an AAc grafting of 20%(V/V). In Fig. 4 it is possible to observe that the Cs immobilization on the PP surface changed its morphology. For lower Cs concentrations (Fig. 4B and 4C), the crystallite boundaries observed on untreated PP surface became almost unnoticeable, indicating that

a kind of continuous, uniform and smooth film may be above it, what may also be observed in Fig. 5B and 5C of profilometry analysis. In more detail for 0.8%Cs, in Fig. 4C, the boundaries really disappeared, which may indicate an increase in that film thickness comparing to 0.4%Cs, achieved by more Cs immobilized on the surface. As indicated by profilometry analysis, the PP surface roughness (R_a value) for these two concentrations is almost the same as in the case of untreated PP. However, when the Cs concentration increases (2%, 4% and 6%(w/V), the R_a value also increases, being possible to observe a rougher surface with more protuberances. This is in accordance with what is possible to observe in Fig. 4D and 4E, where some agglomerates are observed above such film, mainly for the highest Cs concentration, probably being Cs based agglomerates. Saxena et al. also observed similar changes in PP surface morphology when increasing the Cs content immobilized on it [10]. Moreover, these results are in accordance with the acid orange and FTIR-ATR results, namely the fact that using a higher Cs solution concentration leads to more Cs immobilized on PP surface.

Regarding the wettability of Cs treated PP, as presented in Fig. 2B, the biggest water C.A. decrease (about 36.5%) attained for PP_20% AAc_2% Cs, maybe mainly explained by the presence of -OH polar groups from Cs on the PP surface [22]. In addition, the $-NH_2$ groups from Cs that may be present on the surface also have a hydrophilic character [36]. When the Cs is immobilized on PP surface some of its $-NH_2$ groups are involved in $-CONH-$ bonds forming amides, but other ones still in their amine state, creating a more hydrophilic surface as previously mentioned. Therefore, it would be expected that the samples treated with higher Cs solution concentrations showed more -OH and $-NH_2$ groups on their surface and consequently lower water C.A. values. However, for Cs concentrations higher than 2%(w/V) the water C.A. was kept the same, meaning that the quantity of Cs immobilized on the surface did not increase in proportion to the solution concentration. But this phenomenon is in accordance to what was already discussed for the acid orange absorbance results. Besides that, once again it must be noticed that the increase in surface roughness when the Cs is immobilized on PP surface may also be responsible for the hydrophobicity decrease, according to Wenzel's model.

Attending to the main purpose of this work, namely to improve the bioactivity of PP surfaces, the viability and morphology of cells seeded on untreated PP and PP_20% AAc_2% Cs were evaluated. Cell attachment, adhesion, and spreading are very important steps for a good cell/ material interaction. The way these phenomena occur influences the cell's ability to proliferate and to differentiate, which is essential for the formation of an implant/tendon successful interface. Therefore, SEM analysis was performed in order to observe cell adhesion to the Cs treated surface as well as their morphology. As observed in Fig. 7, the cell adhesion occurred and the fibroblasts number increased over time for both tested materials. After 1 day, the cells presented different morphologies comparing the untreated with the treated samples. In the case of Cs treated PP samples (Fig. 7A1), cells are more spread than in the case of untreated PP (Fig. 7A1). After 7 days both materials surfaces was completely covered by a cell layer (Fig. 7A2 and B2), being all cells completely spread and interconnected as a whole surrounded by ECM, but in case of untreated PP it is still possible to observe few cells with a shape not so well spread. At the beginning of the cell adhesion process, if cells present a spherical shape it indicates an initial stage of adhesion or that they are not so well adapted whereas a spread shape reveals a better adaptation and a more advanced adhesion stage [23 37]. In a cell adhesion process, the material interacts with different cell surface receptors, establishing several sites of adhesion between the cells and the material surface [38,39]. During the establishment of those sites, there is an organization and/or production of the

cytoskeleton filamentous proteins, namely actin filaments, which tend to assemble in long bundles, leading to a spread shape with protrusions (filopodia) of the plasma membrane [23,40,41].

Resazurin is an indicator of cell viability since the living cells are able to reduce the resazurin in mitochondria. Therefore the fluorescence results presented in Fig. 6 are proportional to cell metabolism and therefore cell proliferation and viability [42]. After 1 and 3 days of culture, the treated samples present a higher metabolic activity than the untreated ones. However, after 7 days the fluorescence level of the treated samples decrease, probably due to the lack of space for cell proliferation, leading to the detachment of part of the cell layer as proved by optical microscopy (Fig. 6D). The cell shape, which is controlled by the cytoskeleton organization, can also be related to cell growth and function once the cytoskeleton proteins are involved in signal transduction. So, when cells try to adhere to a material surface, the mitochondrial activity increases by the production of the necessary energy to synthesize the above-mentioned proteins [23,35,43]. Therefore, a cell shape more spread and a high number of cells is usually associated with a high metabolic activity, as verified when comparing the SEM images and resazurin fluorescence levels of tested materials after 1 day of culture.

The biomaterial surface characteristics, such as morphology and physical and chemical features influence cell growth and function [44]. For instance, the materials' surface roughness and wettability can influence the type and the adsorption kinetics of the serum proteins to the material surface. The adsorbed protein layer has an essential role in the cell adhesion, morphology, and migration, because the charged cell membrane interacts with surfaces through this protein layer [37,45]. It has been reported in several studies that rough, enough hydrophilic and functionalized surfaces favor the adsorption of that protein layer and consequently the cell adhesion [13,22,33]. Thus, the low cell adhesion and metabolic levels in case of untreated PP may be explained by the lack of functional groups, low wettability, and flat surface. In case of Cs treated samples, the high cell adhesion and activity may be mostly explained by the performed amine functionalization. The several $-NH_2$ groups present on the material surface present positive charges which are able to establish electrostatic interactions with negative charges of the cell-surface proteins, promoting the adhesion of cells to the material [22,33]. Besides that, the cell anchorage may also be improved by the wettability, roughness and topography of the Cs treated PP surface.

Conclusions

Firstly, it was verified that the plasma treatments performed on PP surface improved its wettability and activated the surface, allowing a successful AAc grafting and consequent Cs immobilization. This achievement was proved by the Orange II dye method and by the appearance of new amine and amide peaks on FTIR-ATR spectra when using O_2 plasma. It must be noticed, that as the Cs solution concentration increase the quantity of Cs immobilized on the surface also increases as expect, however after 2%(V/V) it remains constant. Due to the different results obtained in acid orange absorbance test and FTIR-ATR analysis, the plasma using only O_2 and the AAc concentration of 20% were chosen for further characterization. Based on SEM, optical profilometry and water C.A. analysis, it was possible to observe that the Cs concentration increase leads to a surface roughness (R_a value) increase, as well as to water contact angle decrease at least until 2%(w/V). Finally, the substrate PP_20% AAc_2% Cs was chosen to study the cellular

response to the developed Cs immobilized PP surfaces. Thus, resazurin and SEM analysis were performed in order to analyze cell adhesion, proliferation, and morphology. The Cs treated PP revealed better results than the untreated PP, promoting higher cell metabolic activity than the untreated samples. Moreover, SEM results corroborate this conclusion, since cells were spread through the surface indicating a good adhesion and cell growth occurred being the surface all covered by cells on day 7 .

Acknowledgments

Authors acknowledge the financial support from FCT (Fundação para a Ciência e a Tecnologia), through the Grant SFRH/BD/88829/2012 and the Project UIDB/50006/2020.

References

[1] L. Lidgren, E. Gomez-Barrena, G. Duda, W. Puhl, A. Carr, European musculoskeletal health and mobility in Horizon 2020, Bone Joint Res. 3 (2014) 48-50.
[2] M.T. Rodrigues, R.L. Reis, M.E. Gomes, Engineering tendon and ligament tissues: present developments towards successful clinical products, J.Tissue Eng. Regen. Med. 7 (2013) 673-686.
[3] R. James, G. Kesturu, G. Balian, A.B. Chhabra, Tendon: biology, biomechanics, repair, growth factors, and evolving treatment options, J. Hand Surg. 33 (2008) 102-112.
[4] U.G. Longo, A. Lamberti, N. Maffulli, V. Denaro, Tendon augmentation grafts: a systematic review, Br. Med. Bull. 94 (2010) 165-188.
[5] J. Chen, J. Xu, A. Wang, M. Zheng, Scaffolds for tendon and ligament repair: review of the efficacy of commercial products, Expet Rev. Med. Dev. 6 (2009) 61-73.
[6] P. Pedrosa, J.M. Chappé, C. Fonseca, A.V. Machado, J.M. Nóbrega, F. Vaz, Plasma surface modification of polycarbonate and poly (propylene) substrates for biomedical electrodes, Plasma Process. Polym. 7 (2010) 676-686.
[7] M.F. Maitz, Applications of synthetic polymers in clinical medicine, Biosurf. Biotribiol. 1 (2015) 161-176, 1.
[8] T. Guoliang, G. Aijun, L. Jianjun, S. Hung-Jue, D. Bergbreiter, Surface functionalized Polypropylene: synthesis, characterization, and adhesion properties, Macromolecules 34 (2001) 7672-7679.
[9] M. Hara, S. Kitahata, K. Nishimori, et al., Surface-functionalization of isotactic polypropylene via dip-coating with a methacrylate-based terpolymer containing perfluoroalkyl groups and poly(ethylene glycol), Polym. J. 51 (2019) 489-499.
[10] S. Saxena, A.R. Ray, A. Kapil, G. Pavon-Djavid, D. Letourneur, B. Gupta, et al., Development of a new polypropylene-based suture: plasma grafting, surface treatment, characterization, and biocompatibility studies, Macromol. Biosci. 11 (2011) 373-382.
[11] O.-J. Kwon, S.-W. Myung, C.-S. Lee, H.-S. Choi, Comparison of the surface characteristics of polypropylene films treated by Ar and mixed gas (Ar/O 2) atmospheric pressure plasma, J. Colloid Interface Sci. 295 (2006) 409-416.
[12] N. Tang, Q. Jia, H. Zhang, J. Li, S. Cao, Preparation and morphological characterization of narrow pore size distributed polypropylene hydrophobic membranes for vacuum membrane distillation via thermally induced phase separation, Desalination 256 (2010) 27-36.
[13] P. Alves, S. Pinto, H.C. de Sousa, M.H. Gil, Surface modification of a thermoplastic polyurethane by low-pressure plasma treatment to improve hydrophilicity, J. Appl.

Polym. Sci. 122 (2011) 2302-2308.
[14] N. Sanbhal, X. Saitaer, M. Peerzada, A. Habboush, F. Wang, L. Wang, One-step surface functionalized hydrophilic polypropylene meshes for hernia repair using bio-inspired polydopamine, Fibers 7 (2019) 6.
[15] A. Contreras-García, E. Bucio, A. Concheiro, C. Alvarez-Lorenzo, Surface functionalization of polypropylene devices with hemocompatible DMAAm and NIPAAm grafts for norfloxacin sustained release, J. Bioact. Compat Polym. 26 (4) (2011) 405-419.
[16] D.S. Morais, J. Torres, R.M. Guedes, et al., Current approaches and future trends to promote tendon repair, Ann. Biomed. Eng. 43 (2015) 2025-2035.
[17] X. Zhou, F. Wang, Y. Ji, W. Chen, J. Wei, Fabrication of hydrophilic and hydrophobic sites on polypropylene nonwoven for oil spill cleanup: two dilemmas affecting oil sorption, Environ. Sci. Technol. 50 (2016) 3860-3865.
[18] C. Labay, C. Canal, M. García-Celma, Influence of corona plasma treatment on polypropylene and polyamide 6.6 on the release of a model drug, Plasma Chem. Plasma Process. 30 (2010) 885-896.
[19] J.M. Grace, L.J. Gerenser, Plasma treatment of polymers, J. Dispersion Sci. Technol. 24 (2003) 305-341.
[20] C.A. Custódio, C. Alves, R. Reis, J. Mano, Immobilization of fibronectin in chitosan substrates improves cell adhesion and proliferation, J.Tissue Eng. Regen. Med. 4 (2010) 316-323.
[21] K.S. Siow, L. Britcher, S. Kumar, H.J. Griesser, Plasma methods for the generation of chemically reactive surfaces for biomolecule immobilization and cell colonization-A review, Plasma Process. Polym. 3 (2006) 392-418.
[22] L. Tang, P. Thevenot, W. Hu, Surface chemistry influences implant biocompatibility, Curr. Top. Med. Chem. 8 (2008) 270-280.
[23] D. Morais, M. Rodrigues, M. Lopes, M. Coelho, A.C. Maurício, R. Gomes, et al., Biological evaluation of alginate-based hydrogels, with antimicrobial features by Ce (III) incorporation, as vehicles for a bone substitute, J. Mater. Sci. Mater. Med. 24 (2013) 2145-2155.
[24] N. Bhattarai, J. Gunn, M. Zhang, Chitosan-based hydrogels for controlled, localized drug delivery, Adv. Drug Deliv. Rev. 62 (2010) 83-99.
[25] S.C. Ugbolue, Polyolefin Fibres: Industrial and Medical Applications, Elsevier, United Kingdom, 2009.
[26] F. Leroux, A. Perwuelz, C. Campagne, N. Behary, Atmospheric air-plasma treatments of polyester textile structures, J. Adhes. Sci. Technol. 20 (2006) 939-957.
[27] R. Morent, N. De Geyter, C. Leys, L. Gengembre, E. Payen, Comparison between XPS- and FTIR-analysis of plasma-treated polypropylene film surfaces, Surf. Interface Anal. 40 (2008) 597-600.
[28] G. Wolansky, A. Marmur, Apparent contact angles on rough surfaces: the Wenzel equation revisited, Colloid. Surface. Physicochem. Eng. Aspect. 156 (1999) 381-388.
[29] P. Pedrosa, P. Fiedler, C. Lopes, E. Alves, N.P. Barradas, J. Haueisen, et al., Ag: TiNcoated polyurethane for dry biopotential electrodes: from polymer plasma interface activation to the first EEG measurements, Plasma Process. Polym. 13 (3) (2015) 341-354.
[30] R. De Oliveira, D. Albuquerque, F. Leite, F. Yamaji, T. Cruz, Measurement of the Nanoscale Roughness by Atomic Force Microscopy: Basic Principles and Applications, INTECH Open Access Publisher, Brazil, 2012.
[31] S. Saxena, A.R. Ray, B. Gupta, Graft polymerization of acrylic acid onto polypropylene monofilament by RF plasma, J. Appl. Polym. Sci. 116 (2010) 2884-2892.
[32] S. Anjum, A. Gupta, D. Sharma, S. Kumari, P. Sahariah, J. Bora, et al., Antimicrobial nature and healing behavior of plasma functionalized polyester sutures, J. Bioact. Compat Polym. (2016), 0883911516668665.

[33] H.-L. Li, H. Zhang, H. Huang, Z.-Q. Liu, Y.-B. Li, H. Yu, et al., The effect of amino density on the attachment, migration, and differentiation of rat neural stem cells in vitro, Mol. Cell. 35 (2013) 436-443.
[34] N. Sheppard, The Historical Development of Experimental Techniques in Vibrational Spectroscopy, Wiley Online Library, 2002.
[35] H.-X. Sun, L. Zhang, H. Chai, H.-L. Chen, Surface modification of poly (tetrafluoroethylene) films via plasma treatment and graft copolymerization of acrylic acid, Desalination 192 (2006) 271-279.
[36] P. Hamerli, T. Weigel, T. Groth, D. Paul, Surface properties of and cell adhesion onto allylamine-plasma-coated polyethylenterephtalat membranes, Biomaterials 24 (2003) 3989-3999.
[37] D. Morais, S. Fernandes, P. Gomes, M. Fernandes, P. Sampaio, M. Ferraz, et al., Novel cerium doped glass-reinforced hydroxyapatite with antibacterial and osteoconductive properties for bone tissue regeneration, Biomed. Mater. 10 (2015), 055008.
[38] K.J. Zaleski, T. Kolodka, C. Cywes-Bentley, R.M. McLoughlin, M.L. Delaney, B. T. Charlton, et al., Hyaluronic acid binding peptides prevent experimental staphylococcal wound infection, Antimicrob. Agents Chemother. 50 (2006) 3856-3860.
[39] Y. Lei, S. Gojgini, J. Lam, T. Segura, The spreading, migration and proliferation of mouse mesenchymal stem cells cultured inside hyaluronic acid hydrogels, Biomaterials 32 (2011) 39-47.
[40] U. Hempel, T. Hefti, P. Dieter, F. Schlottig, Response of human bone marrow stromal cells, MG-63, and SaOS-2 to titanium-based dental implant surfaces with different topography and surface energy, Clin. Oral Implants Res. 24 (2013) 174-182.
[41] P. Wutticharoenmongkol, P. Pavasant, P. Supaphol, Osteoblastic phenotype expression of MC3T3-E1 cultured on electrospun polycaprolactone fiber mats filled with hydroxyapatite nanoparticles, Biomacromolecules 8 (2007) 2602-2610.
[42] J. O'Brien, I. Wilson, T. Orton, F. Pognan, Investigation of the Alamar Blue (resazurin) fluorescent dye for the assessment of mammalian cell cytotoxicity, Eur. J. Biochem. 267 (2000) 5421-5426.
[43] D.S. Morais, J. Coelho, M.P. Ferraz, P.S. Gomes, M.H. Fernandes, N.S. Hussain, et al., Samarium doped glass-reinforced hydroxyapatite with enhanced osteoblastic performance and antibacterial properties for bone tissue regeneration, J. Mater. Chem. B 2 (2014) 5872-5881.
[44] T.G. Vladkova, Surface engineered polymeric biomaterials with improved biocontact properties, Int. J. polym.Sci. 32 (3) (2010) 263-279.
[45] C.J. Wilson, R.E. Clegg, D.I. Leavesley, M.J. Pearcy, Mediation of biomaterial-cell interactions by adsorbed proteins: a review, Tissue Eng. 11 (2005) 1-18.